

Article

Total Flavonoids from *Camellia oleifera* Alleviated *Mycoplasma pneumoniae*-Induced Lung Injury via Inhibition of the TLR2-Mediated NF- κ B and MAPK Pathways

 Nan Ding ¹, Aihua Lei ¹, Zhisheng Shi ¹, Lin Xiang ¹, Bo Wei ^{2,*} and Yimou Wu ^{1,*}

¹ Hunan Provincial Key Laboratory for Special Pathogens Prevention and Control, Hunan Province Cooperative Innovation Center for Molecular Target New Drug Study, Institute of Pathogenic Biology, Hengyang Medical College, University of South China, Hengyang 421001, China; leiaihua18@usc.edu.cn (A.L.)

² Research Lab of Translational Medicine, Hengyang Medical College, University of South China, Hengyang 421001, China

* Correspondence: usc-wb@usc.edu.cn (B.W.); yimouwu@sina.com (Y.W.)

Abstract: *Mycoplasma pneumoniae* (*M. pneumoniae*) is an atypical bacterial pathogen responsible for community-acquired pneumonia primarily among school-aged children and young adults. *Camellia oleifera* (*C. oleifera*) has been used as a medicinal and edible plant in China for centuries, the constituents from which possessed various bioactivities. Notably, flavonoids existing in residues of *C. oleifera* defatted seeds exhibited significant anti-inflammatory activities. In the present study, we investigated the impact of total flavonoids from *C. oleifera* (TFCO) seed extract on *M. pneumoniae* pneumonia. TFCO was obtained using multiple column chromatography methods and identified as kaempferol glycosides via UPLC-HRESIMS. In a *M. pneumoniae* pneumonia mouse model, TFCO significantly reduced the lung damage, suppressed IL-1 β , IL-6, and TNF- α production, and curbed TLR2 activation triggered by *M. pneumoniae*. Similarly, in RAW264.7 macrophage cells stimulated by lipid-associated membrane proteins (LAMPs), TFCO suppressed the generation of proinflammatory cytokines and TLR2 expression. Moreover, TFCO diminished the phosphorylation of I κ B α , JNK, ERK, p38, and p65 nuclear translocation in vitro. In conclusion, TFCO alleviated *M. pneumoniae*-induced lung damage via inhibition of TLR2-mediated NF- κ B and MAPK pathways, suggesting its potential therapeutic application in *M. pneumoniae*-triggered lung inflammation.

Keywords: flavonoids; *Mycoplasma pneumoniae*; *Camellia oleifera*; TLR2; NF- κ B; MAPK



Citation: Ding, N.; Lei, A.; Shi, Z.; Xiang, L.; Wei, B.; Wu, Y. Total Flavonoids from *Camellia oleifera* Alleviated *Mycoplasma pneumoniae*-Induced Lung Injury via Inhibition of the TLR2-Mediated NF- κ B and MAPK Pathways. *Molecules* **2023**, *28*, 7077. <https://doi.org/10.3390/molecules28207077>

Academic Editors: Irwin Rose
Alencar Menezes, Henrique Douglas
Melo Coutinho, Almir
Gonçalves Wanderley and
Jaime Ribeiro-Filho

Received: 14 September 2023
Revised: 5 October 2023
Accepted: 6 October 2023
Published: 13 October 2023



Copyright: © 2023 by the authors. Licensee MDPI, Basel, Switzerland. This article is an open access article distributed under the terms and conditions of the Creative Commons Attribution (CC BY) license (<https://creativecommons.org/licenses/by/4.0/>).

1. Introduction

Mycoplasma pneumoniae (*M. pneumoniae*) stands out as an atypical bacterial pathogen, manifesting primarily as the lead agent for community-acquired pneumonia (CAP) among school-aged children and young adults [1]. *M. pneumoniae* prompts inflammation in the upper and lower respiratory tracts and contributes to a broad spectrum of extrapulmonary syndromes [2–5]. Accumulating evidence has confirmed that *M. pneumoniae*-induced pneumonia is closely associated with an elevated production of proinflammatory cytokines, including tumor necrosis factor- α (TNF- α) and interleukin- (IL-) 1 β and IL-6. These molecules are not merely byproducts but central actors that cause a series of complex immune events. Their mobilization and activation of an array of leukocytes, such as macrophages and neutrophils, can be a double-edged sword—while they mount a defense against invading pathogens, they can also perpetrate tissue damage if not properly regulated [6,7].

Proinflammatory cytokine secretion during *M. pneumoniae* infection correlates with various immune cells, particularly macrophages [8–10]. The unusual feature of *M. pneumoniae*—its absence of a cell wall—places the lipid-associated membrane proteins (LAMPs) under the investigative spotlight [7]. These surface proteins, integral to *M. pneumoniae*'s

identity, can readily bind to the Toll-like receptor 2 (TLR2) on immune cells, unleashing a cascade of intracellular events [7,11,12]. This involves the activation of signaling pathways like NF- κ B and MAPK, which act as conduits to produce a plethora of proinflammatory cytokines [7,13,14]. These pathways, while vital for immune responses, also underscore the delicate balance that needs to be maintained to prevent overactive inflammation [7].

Camellia oleifera (*C. oleifera*), a botanical treasure native to regions of central and southern China, has historically been more than just a plant. Its seeds have served in high-quality oil production for centuries. *C. oleifera* by-products, such as camellia seed cake and fruit shell, are extensively used in the dyeing, papermaking, chemical fiber, textile, organic fertilizer, detergent, and pesticide industries [15,16]. Beyond its industrial utility, contemporary research has ventured into tapping its therapeutic potential. The residual defatted seed pomace of *C. oleifera* is rich in bioactive substances, predominantly flavonoids [17–21], saponins [22,23], and polysaccharides [24,25]. Among these, flavonoids, principally kaempferol glycosides, manifest a broad spectrum of biological activities, encompassing anti-inflammation [20,21,26], anti-oxidation [26,27], anti-melanogenesis [27], and anti-microbial [28] activities.

Prior research indicated that *C. oleifera* defatted seed extracts exhibited notable anti-inflammatory activities in vivo, mitigating carbon tetrachloride-induced hepatotoxicity and nonalcoholic fatty liver disease in rats [29,30]. Furthermore, the flavonoids present in the residues of *C. oleifera* defatted seeds inhibited NO and proinflammatory cytokine production in LPS-stimulated RAW264.7 macrophages, chiefly by suppressing the NF- κ B signaling pathway [20,21].

Given this context, we first postulated that the total flavonoids from the extract of defatted *C. oleifera* (TFCO) seeds might alleviate *M. pneumoniae*-induced pneumonia. This study not only corroborates our hypothesis but also delves into molecular intricacies to elucidate the inherent mechanisms.

2. Results

2.1. The Major Components of TFCO

Five compounds (1–5) were detected in TFCO by UPLC–HRESIMS and numbered according to the elution order (Figure 1A). The negative HRESIMS for compounds 1–5 displayed signals at 755.2136, 739.2149, 725.2098, 797.2225, 767.2036, respectively (Figure 1B). ^1H NMR (600 MHz) and ^{13}C NMR (150 MHz) data for compounds 1 and 3 were consistent with corresponding data reported in the literature (Table S1, Figures S1–S4) [17,18]. The fragment ions at m/z 285 indicated the aglycone was kaempferol. These results align with previous reports. Thus, compounds 1–5 were confirmed as kaempferol-3-O-[2-O- β -D-glucopyranosyl-6-O-L-rhamnopyranosyl]- β -D-glucopyranoside (compound 1) [17,18,20], kaempferol-3-O- β -D-glucopyranosyl-(1 \rightarrow 4)- α -L-rhamnopyranosyl-7-O- α -L-rhamnopyranoside (compound 2) [20,31], kaempferol-3-O-[2-O- β -D-xylopyranosyl-6-O- α -L-rhamnopyranosyl]- β -D-glucopyranoside (compound 3) [17,18,20], kaempferol-3-O-[4'''-O-acetyl- α -L-rhamnopyranosyl-(1 \rightarrow 6)]- β -D-glucopyranosyl-(1 \rightarrow 2)]- β -D-glucopyranoside (compound 4) [19], kaempferol-3-O-[4'''-O-acetyl- α -L-rhamnopyranosyl-(1 \rightarrow 6)]- β -D-xylopyranosyl-(1 \rightarrow 2)]- β -D-glucopyranoside (compound 5) (Figure 1C) [19]. The UPLC chromatogram revealed that compounds 1–5 accounted for 39.44%, 3.78%, 52.95%, 1.31%, and 0.96%, respectively, with a total percentage of 98.44%. The yield and % yield (w/w) of TFCO and compounds 1–5 from *C. oleifera* are listed in Table S2. This suggested that the five kaempferol glycosides were the major constituents present in TFCO.

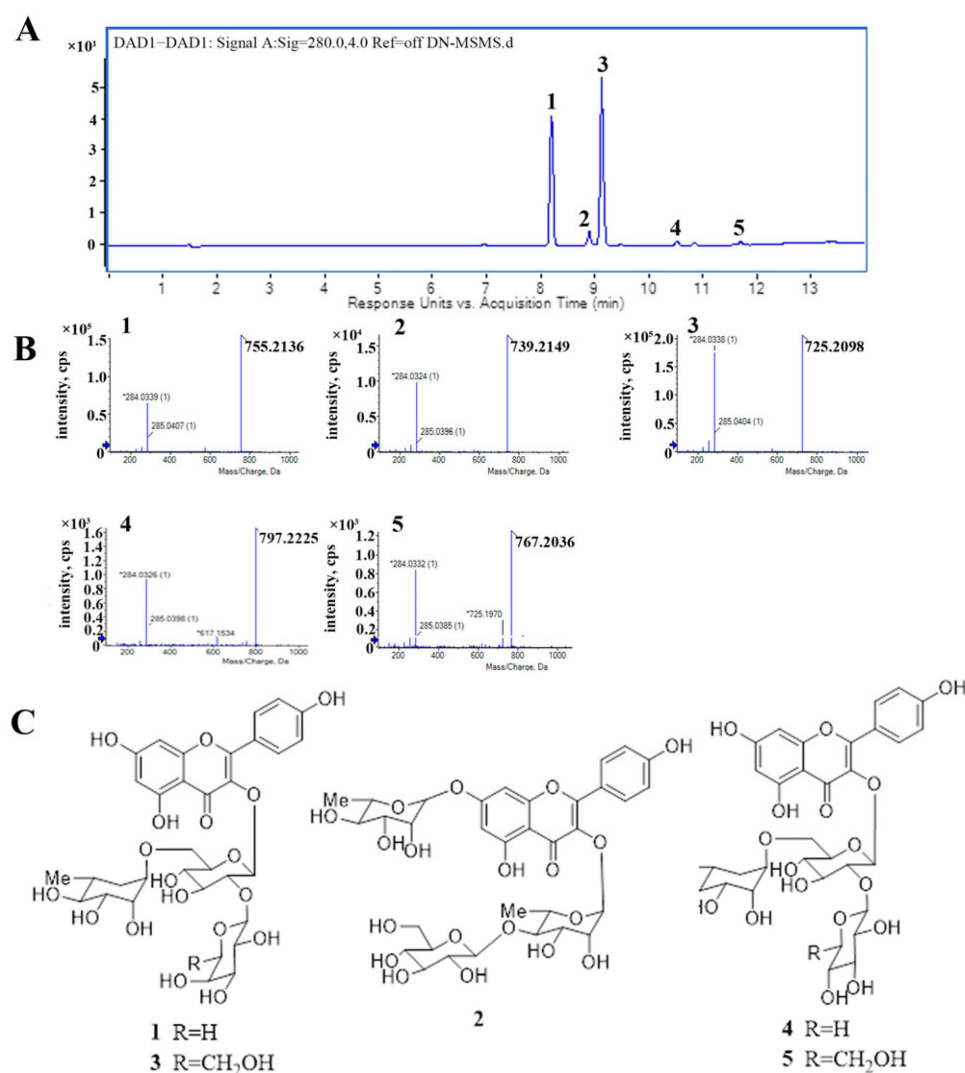


Figure 1. Flavonoids in TFCO. (A) UPLC analysis of flavonoids from TFCO; (B) HRESIMS spectra of the five kaempferol glycosides from TFCO; (C) structures of the five kaempferol glycosides from TFCO.

2.2. TFCO Alleviated Pathological Changes in *M. pneumoniae*-Induced Lung Injury in Mice

The lung sections stained with *Hematoxylin and Eosin* (HE) are shown in Figure 2. No pathological lesions were observed in lung tissues from the control group (Figure 2A) or the TFCO group (Figure 2B). In mice infected with *M. pneumoniae*, lung tissues exhibited significant pathological alterations, including looser alveolar structures, prominent inflammatory cell infiltration, thickened alveolar walls, and narrowed bronchial tubes (Figure 2C). These pathological changes were markedly improved by TFCO administration in a dose-dependent manner (Figure 2D,E). The histology score also indicated that TFCO, isolated from the *C. oleifera* seed extract, could alleviate lung tissue injury caused by *M. pneumoniae* infection (Figure 2F).

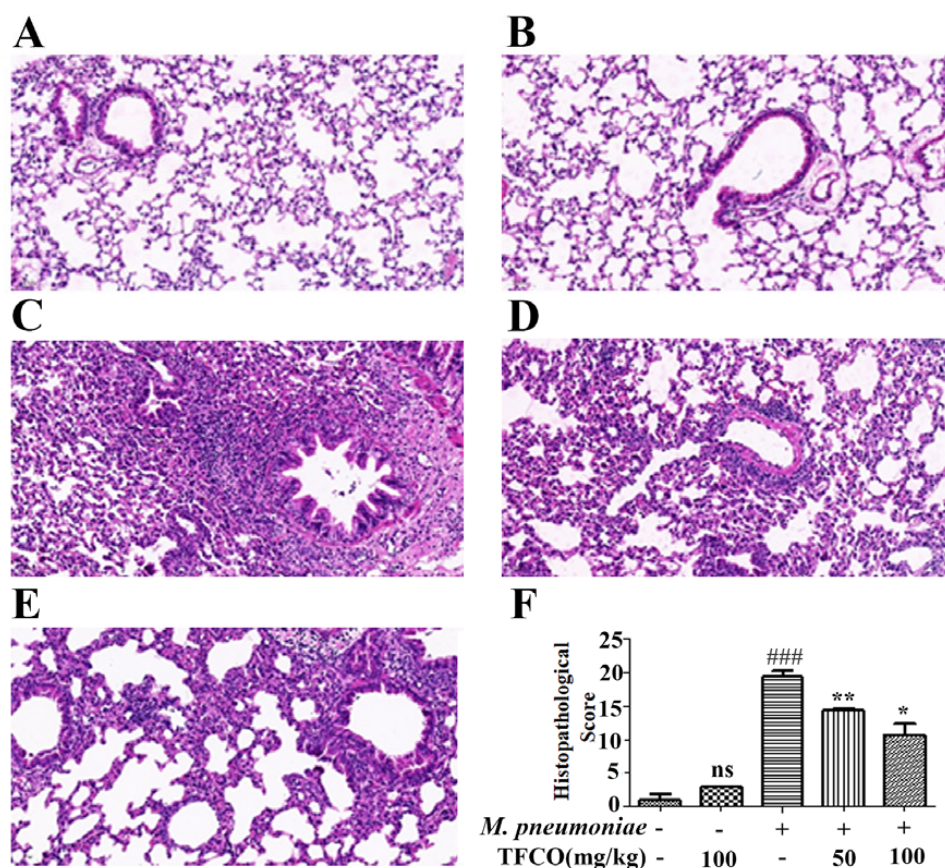


Figure 2. Effects of TFCO on *M. pneumoniae*-induced lung injury. $n = 5$ (A) control group; (B) TFCO (100 mg/kg) group; (C) *M. pneumoniae* group; (D,E) *M. pneumoniae* + TFCO (50 and 100 mg/kg) groups. (Magnification $\times 20$). (F) histopathological scores. ns: non-significant differences, ### $p < 0.001$ versus the control group; * $p < 0.05$, ** $p < 0.01$ versus *M. pneumoniae* group.

2.3. TFCO Suppressed Pro-Inflammatory Cytokines Secretion in *M. pneumoniae*-Infected Mice and LAMPs-Stimulated RAW264.7 Cells without Affecting Cell Viability

M. pneumoniae-infected mice were analyzed for contents of pro-inflammatory cytokines in the bronchoalveolar lavage fluid (BALF). TNF- α , IL-1 β , and IL-6 levels in the *M. pneumoniae* infection group were significantly higher compared to the control group. Treatment with TFCO at 100 mg/kg did not influence TNF- α , IL-1 β , and IL-6 levels. In contrast, the content of these pro-inflammatory mediators induced by *M. pneumoniae* infection was markedly decreased by treatment with TFCO at 50 and 100 mg/kg in a dose-dependent manner (Figure 3A). Additionally, ELISA assays demonstrated that TFCO could dose-dependently alleviate the increased TNF- α , IL-1 β , and IL-6 levels in the supernatants of LAMPs-stimulated RAW264.7 cells (Figure 3B), while working concentrations of TFCO at 25 and 50 $\mu\text{g}/\text{mL}$ had no influence on the cell viability of RAW264.7 cells (Figure 3C).

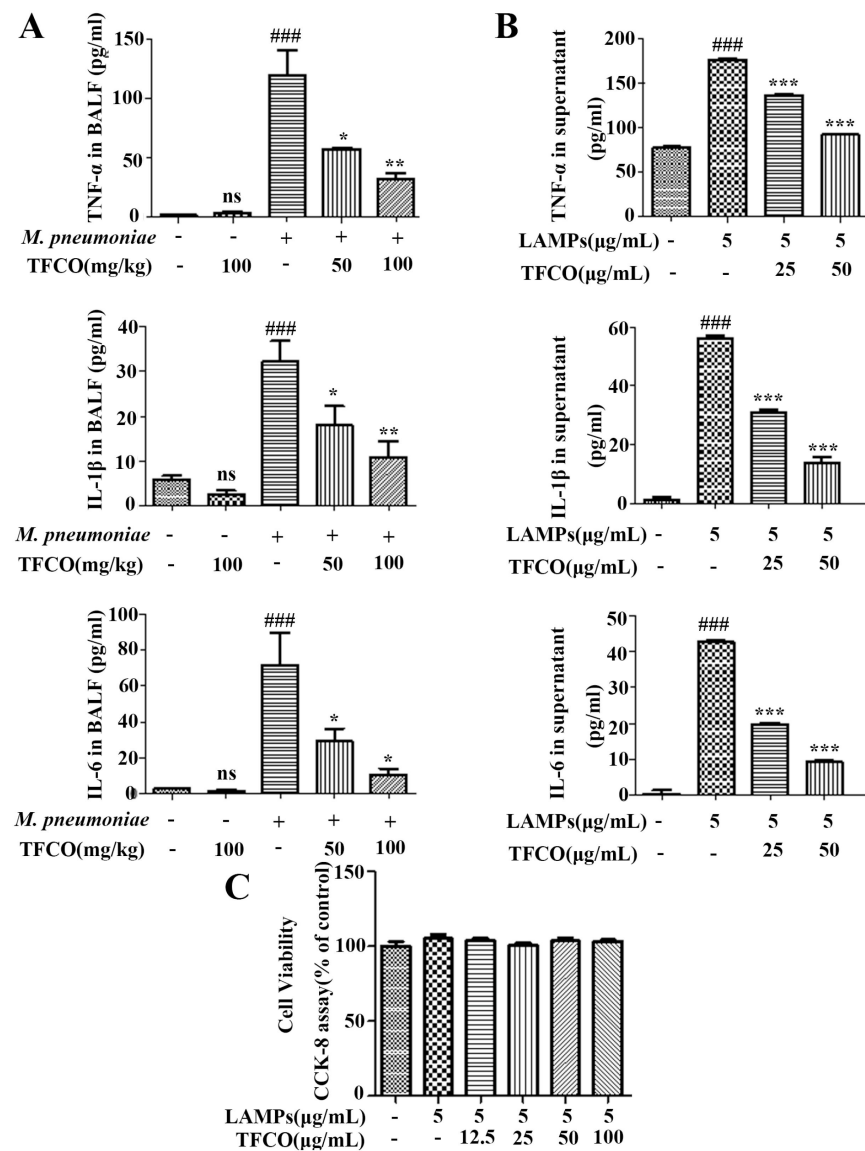


Figure 3. Effects of TFCO on pro-inflammatory cytokines. (A) TNF- α , IL-1 β , and IL-6 level in BALF of Balb/c mice ($n = 5$). (B) TNF- α , IL-1 β , and IL-6 level in the supernatants of RAW264.7 cells ($n = 3$). (C) cell viability of RAW264.7 cells treated with different concentration of TFCO ($n = 3$). ns: non-significant differences, ### $p < 0.001$ versus control group; * $p < 0.05$, ** $p < 0.01$, *** $p < 0.001$ versus model group.

2.4. TFCO Suppressed TLR2 Expression in *M. pneumoniae*-Infected Mice and LAMPs-Stimulated RAW264.7 Cells

The level of TLR2 protein in mice lung tissues was detected using immunofluorescence staining, which indicated that TLR2 expression in mice lung tissue in the control group and TFCO-treated group was low. However, it was significantly higher after intranasal infection with *M. pneumoniae* (Figure 4). TFCO treatment could reduce the *M. pneumoniae*-induced increase in TLR2 expression in a dose-dependent manner (Figure 4). TLR2 expression in RAW264.7 cells was measured by immunofluorescence staining and Western blot, which also showed that administration of TFCO could dose-dependently decrease the elevated expression of TLR2 protein in RAW264.7 macrophages caused by LAMPs stimulation (Figure 5).

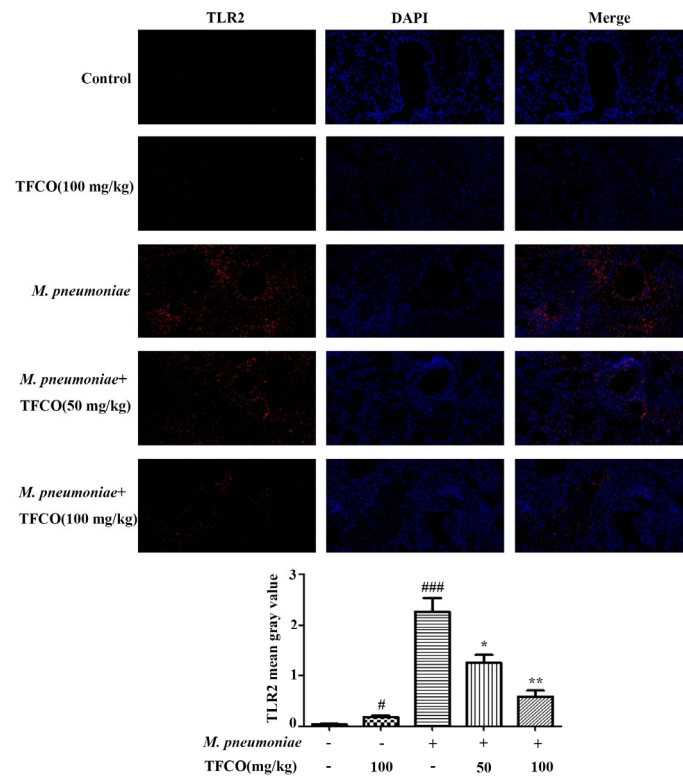


Figure 4. Effects of TFCO on TLR2 in the lung of *M. pneumoniae*-infected Balb/c mice. $n = 5$. Immunofluorescence: DAPI stained blue dots represent nuclei, and the red dots represent TLR2 (Magnification $\times 20$). # $p < 0.05$, ### $p < 0.001$ versus ctrl group; * $p < 0.05$, ** $p < 0.01$ versus *M. pneumoniae* group.

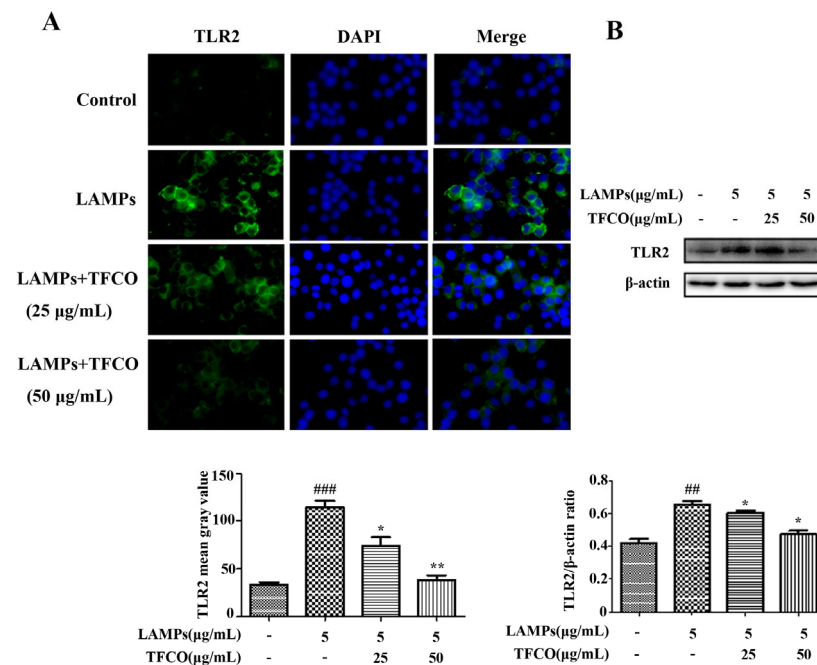


Figure 5. Effects of TFCO on TLR2 in LAMPs-stimulated RAW264.7 cells. (A) immunofluorescence: DAPI stained blue dots represent nuclei, and the green dots represent TLR2 (Magnification $\times 100$). (B) Western blot. $n = 3$. ## $p < 0.01$, ### $p < 0.001$ versus control group; * $p < 0.05$, ** $p < 0.01$ versus LAMPs group.

2.5. TFCO Attenuated the Activation of NF- κ B Pathway in LAMPs-Stimulated RAW264.7 Cells

To further investigate the effects of TFCO on the *M. pneumoniae*-induced NF- κ B signaling pathway, the contents of p-I κ B α proteins in RAW264.7 macrophage cells were detected by Western blot assays. The results indicated that the p-I κ B α proteins were markedly higher in the LAMPs-stimulated group compared to the control group. TFCO treatment dose-dependently reduced the expression of p-I κ B α (Figure 6B). To verify our findings, we observed the nuclear translocation of the NF- κ B p65 protein in RAW264.7 cells using immunofluorescence staining. The results indicated that after TFCO treatment, the nuclear p65 expression was significantly decreased compared to *M. pneumoniae*-challenged cells (Figure 6A).

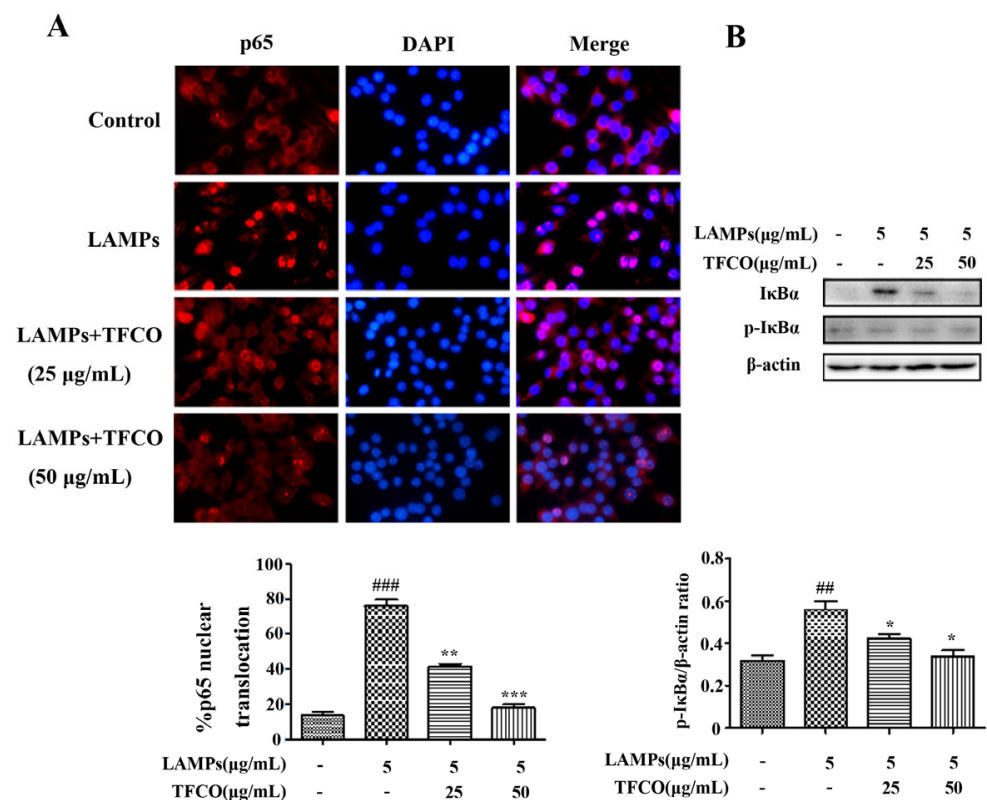


Figure 6. Effects of TFCO on the NF- κ B signaling pathway in LAMPs-stimulated RAW264.7 cells ($n = 3$). (A) the translocation of p65 into nucleus: DAPI stained blue dots represent nuclei, and the red dots represent p65 (Magnification $\times 100$). (B) Western blot: The phosphorylation of I κ B α ; ### $p < 0.01$, ### $p < 0.001$ versus control group; * $p < 0.05$, ** $p < 0.01$, *** $p < 0.001$ versus model group.

2.6. TFCO Inhibited the Activation of MAPK Pathway in LAMPs-Stimulated RAW264.7 Cells

To assess the effect of TFCO treatment on the MAPK signaling pathway, the expression of proteins ERK, JNK, and p38 was determined. Our results revealed that expression levels of phosphorylated ERK, JNK, and p38 proteins were significantly increased in the LAMPs-stimulated group in comparison to the control group. In contrast, the expression of these phosphorylated proteins was significantly reduced by TFCO treatment in a dose-dependent pattern (Figure 7), indicating that TFCO might inhibit the MAPK signaling pathway to alleviate *M. pneumoniae* infection.

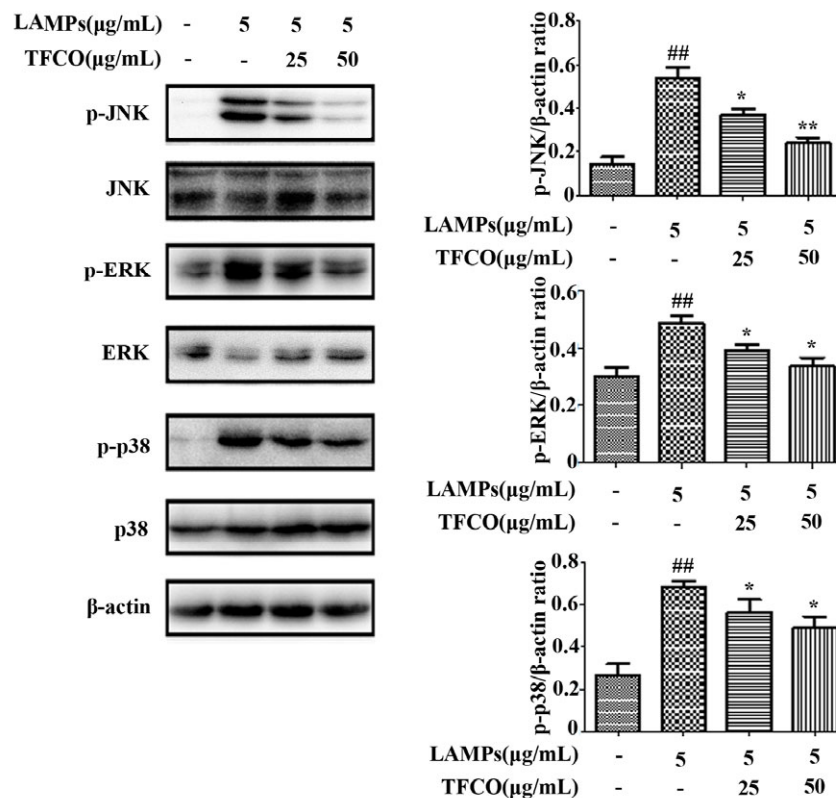


Figure 7. Effects of TFCO on the phosphorylation of MAPK signaling pathway in the LAMPs-stimulated RAW264.7 cells ($n = 3$). ^{##} $p < 0.01$ versus control group; ^{*} $p < 0.05$, ^{**} $p < 0.01$ versus model group.

3. Discussion

M. pneumoniae is an obligate bacterial pathogen, particularly nefarious for its capacity to instigate respiratory diseases. When the epidemiological data are brought under the lens, it is evident that during outbreak seasons, *M. pneumoniae* shoulders the burden for 8% of CAP cases in pediatric populations and notable 2% in adults [32]. These statistics become even more compelling when viewed in a global context; *M. pneumoniae* outbreaks are not confined to specific geographies. Indeed, it has cast its shadow worldwide. Compounding this challenge is the rise of macrolide-resistant *M. pneumoniae* strains. Notably, regions such as Asia, Europe, and North America are sounding alarms with escalating prevalence rates of these resistant strains. Yet, the pathogenic repertoire of *M. pneumoniae* is not restricted merely to the respiratory tract. It is also implicated in a range of extrapulmonary manifestations, including damage to the skin, nervous system, heart, and joints [32].

C. oleifera is a highly valued plant with both medicinal and edible properties. The mature seeds of *C. oleifera* are mainly used for extraction of Camellia oil, which is a pure natural edible oil which has been used for treating gastrointestinal pain and skin burns in people for a long time [26]. The residues of *C. oleifera* seeds are by-products of oil production, traditionally used as animal feed or incinerated for heating. Pharmacological studies have shown that the chemical constituents from the residues of *C. oleifera* seeds possess a variety of biological activities, including anti-inflammation, antioxidation, antitumor, antibacterial, and so on [16,26]. Previous reports had reported that the hot-water extract of defatted *C. oleifera* seeds exerted significant anti-inflammatory effects, providing mild alleviation of hepatic inflammation in CCl_4 -induced liver hepatotoxicity [29]. Kaempferol glycosides, identified as the primary anti-inflammatory flavonoids in *C. oleifera* defatted seeds, have exhibited pronounced anti-inflammatory activity, corroborating our findings [20,21]. These glycosides displayed significant anti-inflammatory effects in mouse asthma [33,34] and rat

transient focal stroke models [35]. In this study, we first investigated the protective effects of kaempferol glycosides against *M. pneumoniae*-induced lung injury in mice.

Immune damage resulting from the excessive secretion of inflammatory factors plays a crucial role in the pathogenesis of *M. pneumoniae* infection. A hallmark of *M. pneumoniae*'s biology is its absence of a traditional cell wall. This anomaly directs attention towards LAMPs anchored in its membrane, which are increasingly recognized as key pathogenic triggers. These proteins interface with TLR2 receptors on monocytes and macrophages, setting off a cascade of immune reactions [7]. This liaison stimulates the copious release of inflammatory mediators, forging a path towards immune-mediated tissue damage [7]. In this study, the in vivo model of *M. pneumoniae* pneumonia was established by infecting mice with *M. pneumoniae* nasal drops [36,37], while the in vitro model was built by stimulating RAW264.7 macrophages with LAMPs.

Several studies have confirmed that the secretion of pro-inflammatory cytokines, such as TNF- α , IL-1 β , and IL-6, is closely related to the severity and outcome of diseases following *M. pneumoniae* infection. Their biphasic role is evident: at physiological levels, they fine-tune immune responses aiding in pathogen elimination; however, when secreted in excess, they can wreak havoc, spurring uncontrolled inflammation, cellular death, and extensive tissue necrosis [38–40]. Previous studies highlighted the substantial inhibitory effects of kaempferol glycosides, isolated from *C. oleifera* defatted seeds and other plants, on the production of proinflammatory cytokines in LPS-activated macrophages [20,21,41,42]. In our investigation, the level of TNF- α , IL-1 β , and IL-6 in the BALF from *M. pneumoniae*-infected mice, as well as in the supernatant from LAMPs-stimulated RAW264.7 macrophages, were notably reduced in the TFCO-treated cohorts compared to the model groups, exhibiting a dose-dependent trend. These findings suggested that the anti-inflammatory effects of TFCO, primarily kaempferol glycosides, may be related to the reduction in pro-inflammatory levels.

TLR is a transmembrane pattern recognition receptor that can be activated by invading pathogens, mediating immune response, and participating in inflammatory reactions. TLR2, as the most crucial pattern recognition receptor for immune system stimulation by *M. pneumoniae*, is the main receptor for LAMPs. However, it cannot recognize LAMPs alone and requires the assistance of other TLRs. Specifically, TLR2 collaborates with TLR1 to recognize triacyl lipoproteins and with TLR6 to recognize diacyl lipoproteins [14,43]. Studies have shown that TLR2 is closely related to lung inflammatory damage caused by *M. pneumoniae* [7,44]. In Balb/c mice infected with *M. pneumoniae*, the activation of TLR2 significantly upregulates the secretion of respiratory mucin [44]. Moreover, after mice have TLR2 knocked out or are intranasally inoculated with TLR2 antibodies, the secretion of inflammatory factors in their BALF is significantly reduced, further indicating that TLR2 activation is an essential factor inducing inflammatory reactions post *M. pneumoniae* infection [44]. In this experiment, following the infection of Balb/c mice with *M. pneumoniae* or stimulation of mouse macrophages RAW264.7 with LAMPs, a noticeable increase was observed in TLR2 protein expression in mouse lung tissues and RAW264.7 cells. After being treated with different concentrations of TFCO, the expression of TLR2 significantly decreased in a dose-dependent manner. Consequently, we posited that TFCO primarily alleviated pulmonary inflammation and damage caused by *M. pneumoniae* infection by inhibiting TLR2 expression.

To further investigate the key mechanisms underlying the anti-inflammatory effects of TFCO, we examined the TLR2-mediated activation of the NF- κ B and MAPK signaling pathways. Both the NF- κ B and MAPK pathways are highly conserved signaling pathways present in all eukaryotes, participating in a wide range of essential cellular physiological and pathological processes, such as regulating cell growth, differentiation, and inflammatory responses. Upon recognition by TLR2, LAMPs can activate NF- κ B and MAPKs to induce the production of various pro-inflammatory cytokines and mediators in immune cells, such as monocytes, macrophages, and natural killer cells, participating in immune responses [45]. The MAPK signaling pathway mainly includes three pathways: JNK, ERK, and p38. Previous literature has shown that in RAW264.7 cells stimulated with *M. pneu-*

moniae extracts or infected with *M. pneumoniae*, all three signaling pathways are activated, which is consistent with our results [12,46]. TFCO treatment remarkably alleviated the phosphorylation of NF- κ B and MAPK signaling pathway proteins both in vivo and in vitro.

While kaempferol glycosides constitute the primary component of TFCO at 98.44%, the potential influence of other active ingredients on the experimental outcomes should not be overlooked. The bioactive compounds in *C. oleifera* defatted seeds predominantly include flavonoids [17–21], saponins [22,23], and polysaccharides [24,25]. Notably, saponins obtained from *C. oleifera* possessed in vivo anti-inflammatory activity [47,48]. While no anti-inflammatory activity has been reported for polysaccharides from *C. oleifera*, the polysaccharides from other plants have shown significant anti-inflammatory properties [49]. Thus, the residual saponins and polysaccharides in TFCO might also contribute to its anti-inflammatory effect on *M. pneumoniae* pneumonia in mice.

Beyond *M. pneumoniae* pneumonia, the total flavonoids from *C. oleifera* defatted seeds might benefit in the treatment of other conditions, particularly those related to TLR2 activation, like sepsis and *Clostridium difficile* infection [50]. Additionally, kaempferol glycosides in TFCO might possess similar effects to their derivatives, which have mitigated inflammation in asthma and stroke in vivo [33,34].

4. Materials and Methods

4.1. Reagents and Antibodies

DMEM, PBS, and fetal bovine serum (FBS) were purchased from Gibco (Grand Island, NY, USA). Rabbit antibodies against TLR2, cy3-conjugated secondary antibody, 4', 6-diamidino-2-phenylindole (DAPI) were purchased from Abcam (Cambridge, UK). Rabbit antibodies against p65, p-I κ B α , I κ B α , p-JNK, JNK, p-ERK, ERK, p-p38, p38, mouse antibody β -actin, and HRP-labeled secondary antibodies were products of Cell Signaling Technology (Beverly, MA, USA). The ELISA assays kit for TNF- α , IL-1 β , and IL-6 were bought from Thermo Fisher (Invitrogen, Waltham, MA, USA). The pleuropneumonia-like organisms (PPLO) broth was obtained from BD Biosciences (Franklin Lake, NJ, USA). Triton X-114 was product of Solarbio (Beijing, China). HRESIMS were measured using AB SCIEX Triple TOF 6600 mass instruments (SCIEX, Framingham, MA, USA). UPLC was performed on Agilent 1290 (Agilent, Palo Alto, CA, USA). Silica gel (200–300 mesh, Qingdao, China), HP-20 macroporous resin (Lupital, Japan) were utilized for column chromatography. Subsequently, ODS column chromatography was applied to obtain compound 1 and compound 3 in TFCO.

4.2. Preparation and UPLC-HRESIMS Analysis of TFCO

Five kilograms of *C. oleifera* seeds, collected from factories in Youxian County, Hunan Province, China, were ground into a powder and defatted using petroleum ether and ethyl acetate [18,21]. Subsequently, TFCO was prepared from the butyl alcohol extract of *C. oleifera* seeds, which was treated with a silica gel (200–300 mesh) column chromatography elution with a gradient CH₂Cl₂-MeOH solvent system (from 10:1 to 1:1, and finally only MeOH), followed by HP-20 macroporous resin eluted with 70% ethanol.

Chromatographic separation of TFCO was conducted on an Acquity HSS T3 C18 column (2.1 mm \times 100 mm, 1.8 μ m, Waters). The gradient elution system comprised solvent A (formic acid/water, 0.5:99.5, *v/v*) and solvent B (acetonitrile) and was set as follows: 0–10 min, 5–25% B; 10–13 min, 25–50% B; 13–14 min, 50–95% B. The flow rate was 0.3 mL/min. The ions of HRESIMS were obtained within the range of *m/z* 100–1500.

4.3. *M. pneumoniae* Culture and Extraction of LAMPs

The *M. pneumoniae* culture and extraction of LAMPs were carried out following previously described methods [28]. Briefly, *M. pneumoniae* strain M129 (ATCC 29342) was cultured in PPLO broth (BD Biosciences) supplemented with 20% FBS, 0.25% glucose, 0.4% yeast extract (Oxoid), penicillin G (1000 U/mL), and phenol red (0.005%) at pH 7.6 and 37 °C for 5–7 days, until the pH indicator transitioned from red to orange. The *M.*

pneumoniae pellet was obtained by centrifugation, resuspended in Tris-buffered saline with 1 mM ethylenediaminetetraacetic, and further dissolved by Triton X-114 (Solarbio, Beijing, China) to a final concentration of 2%. Subsequently, the Triton X-114 lysate was incubated at 37 °C for 10 min to allow phase separation and the underlying Triton X-114 phase was retained. Precipitated protein was obtained by further adding ethanol and centrifugation. Finally, the LAMPs were resuspended in phosphate-buffered saline (PBS) to determine concentration and stored at −20 °C or −80 °C for subsequent experiments.

4.4. Animals and Experimental Design

Specific-pathogen-free Balb/c mice (male, 4 week-old) were acquired from SJA Laboratory Animal Co., Ltd. (Changsha, China) and assigned into five groups ($n = 5$ /group): the control group, the TFCO group (mice treated with 100 mg/kg TFCO only), the *M. pneumoniae* group (*M. pneumoniae*-infected mice), the *M. pneumoniae* + low TFCO group (*M. pneumoniae*-infected mice treated with 50 mg/kg TFCO), and the *M. pneumoniae* + high TFCO group (*M. pneumoniae*-infected mice treated with 100 mg/kg TFCO). Mice in the control and TFCO groups were treated with PPLO using nasal drops, whereas mice in the other groups were intranasally inoculated with 50 μ L *M. pneumoniae* suspension (1×10^8 CFU/mL) for 3 days. Additionally, TFCO was administered by gavage in the TFCO, *M. pneumoniae* + low TFCO, and *M. pneumoniae* + high TFCO groups once at 10 am daily for 7 consecutive days. The control and *M. pneumoniae* groups received intragastric administration of 200 μ L of PBS.

On day 7, mice were euthanized and fixed in a supine position. The lungs were irrigated three times with 0.5 mL of PBS to obtain the BALF for pro-inflammatory cytokines determination. The entire lungs were collected for HE staining and immunohistochemistry. All animal experiments were approved by the University of South China Institutional Animal Use and Ethics Committee (Hengyang, China).

4.5. Cell Culture and Stimulation with LAMPs

The mouse macrophage cell line RAW264.7 was purchased from the Cell Bank of the Chinese Academy of Sciences (Shanghai, China) and cultivated in DMEM (HyClone, Logan, UT, USA) containing 10% FBS, 2 mmol/L L-glutamine, and 100 μ g/mL penicillin/streptomycin. Cells were seeded in 6-well plates at a density of 1×10^6 cells/well. After incubating at 37 °C under 5% CO₂ for 24 h, the TFCO (50 μ g/mL, 25 μ g/mL) was added to the wells and cultured for 1 h. Then, cells were stimulated with or without 5 μ g/mL LAMPs for 24 h.

4.6. Cell Viability Assay

The cytotoxicity of TFCO was assessed using CCK-8 assay. The cells (2×10^5 cells/well) were seeded in 96-well plates and cultured overnight. The cells were incubated for 2 h with or without TFCO (12.5, 25, 50 and 100 μ g/mL) and in the presence or absence of LAMPs (5 μ g/mL). Following a 24 h incubation, 10 μ L of CCK-8 solution was added to each well, and the absorbance optical density (OD) was measured at a wavelength of 450 nm using an enzyme labeling instrument.

4.7. HE Staining

The left lung lobes were fixed with 4% paraformaldehyde, embedded in paraffin, and sectioned. The sections were stained by HE for observation under light microscopy. Lung injury severity was assessed using a semiquantitative histology score through a double-blind method. The histopathological score (HPS) was determined based on the condition of peribronchial or bronchial infiltration, bronchial or bronchial exudate, perivascular and leukocyte infiltration. Each item was assigned a grade ranging from 0 to 3 (0 = no damage; 1 = mild damage; 2 = moderate damage; and 3 = severe damage). The calculated scores were used for statistical analysis.

4.8. Enzyme-Linked Immunosorbent Assay

TNF- α , IL-6, and IL-1 β levels in mouse BALF and the supernatants of RAW264.7 cells were measured using commercially available enzyme immunoassay kits (Invitrogen, Waltham, MA, USA) according to the manufacturer's instructions.

4.9. Immunofluorescence Staining

Lung tissue sections were deparaffinized in xylene and dehydrated with graded ethanol. Heat-mediated antigen retrieval was conducted in EDTA antigen repair buffer (pH 6.0), followed by permeabilization for 10 min with 0.1% Triton X-100, and blockage for 1 h in 5% bovine serum albumin. Subsequently, lung sections were incubated with rabbit antibody against TLR2 at 4 °C overnight, and then stained with Cy3-conjugated goat-anti-rabbit antibody at room temperature for 1 h. After washing in PBS and staining with DAPI, lung sections were examined and images were captured using a fluorescence microscope (Nikon Eclipse C1, Tokyo, Japan).

Mouse RAW264.7 cells were seeded onto coverslips in a 24-well plate. After fixing with 4% PFA for 30 min and permeabilizing with 0.3% Triton X-100 for 10 min, cells were blocked with DMEM containing 10% FBS. Subsequently, the specimens were incubated with primary rabbit antibody against TLR2 and NF- κ B p65 overnight at 4 °C, followed by incubation with Cy3-conjugated goat anti-rabbit antibody for another 1 h. Nuclei were stained with DAPI for 15 min at room temperature and images were acquired using an immunofluorescence microscope (Ts2R, Nikon, Japan).

4.10. Western Blot Analysis

RAW264.7 cells for Western blot assay were collected and lysed by RIPA lysis buffer containing 1% phosphatase and protease inhibitors. Protein content in the samples was measured by BCA protein assay kit. After denaturing in boiling water for 10 min, equal amounts of the total proteins were separated by SDS-PAGE electrophoresis and electro-transferred to PVDF membranes following standard procedures. The membranes were blocked with TBST containing 5% non-fat milk for 2 h at room temperature and incubated with primary antibodies against β -actin, TLR2, p-I κ B α , I κ B α , p-JNK, JNK, p-ERK, ERK, p-p38, and p38 overnight at 4 °C. After washing with TBST five times, HRP-conjugated secondary antibody was added to the membranes for 1 h at 37 °C, followed by further washing with PBS. Immunoreactive bands were visualized using the ECL system (Syngene, G: BOX XX8, Cambridge, UK) and densitometric analysis was quantified using Image J 1.44.

4.11. Statistical Analysis

All experiments were performed independently three times, and the data referenced above were expressed as Mean \pm SEM. GraphPad Prism 5.0 software was used for statistical analysis, and one-way ANOVA was applied to compare different groups. Statistical significance was defined as * $p < 0.05$, ** $p < 0.01$, and *** $p < 0.01$.

5. Conclusions

In summary, our study is the first to investigate the protective effects of kaempferol glycosides, including, but not limited to, those from *C. oleifera* defatted seeds, against *M. pneumoniae*-induced lung damage. The potential mechanism may be associated with the inhibition of TLR2-mediated NF- κ B and MAPK signaling pathways. This research underscored the potential therapeutic value of *C. oleifera*, suggesting its prospective use in treating lung inflammation caused by *M. pneumoniae*.

Supplementary Materials: The following supporting information can be downloaded at: <https://www.mdpi.com/article/10.3390/molecules28207077/s1>. Table S1. ¹H NMR (600 MHz) and ¹³C NMR (150 MHz) data for compounds 1 and 3 in CD₃OD (δ in ppm, J in Hz). Table S2. Contents of TFCO and compounds 1–5 in *Camellia oleifera* seed. Figure S1. The load of *M. pneumoniae* in the lungs

of infected mice. ns: non-significant differences versus *M. pneumoniae* group. Figure S2. The weight of mice. ns: non-significant differences, ** $p < 0.01$. Figure S3. ^1H NMR of compound 1. Figure S4. ^{13}C NMR of compound 1. Figure S5. ^1H NMR of compound 3. Figure S6. ^{13}C NMR of compound 3.

Author Contributions: Methodology, Y.W., N.D. and B.W.; Software, N.D. and B.W.; Validation, A.L.; Formal analysis, N.D.; Investigation, N.D., Z.S. and L.X.; Writing—original draft, N.D. and B.W.; Writing—review and editing, A.L. and Y.W.; Supervision, B.W.; Project administration, B.W. and Y.W.; Funding acquisition, Y.W. All authors have read and agreed to the published version of the manuscript.

Funding: This work was supported by the National Natural Science Foundation of China (grant Nos. 82101869, 81671986, and 31872643), the Natural Science Foundation for Young Scientists of Hunan Province (grant Nos. 2021JJ40471 and 2021JJ40478), the Scientific research project of Hunan Education Department (grant Nos. 21B0404 and 20B506), and the Hunan University students Innovation and Entrepreneurship training program (grant Nos. S202110555319, S202110555105, 2022X10555107, and 2022X10555113).

Institutional Review Board Statement: The animal study protocol was approved by the Ethics Committee of the Animal Experiment Research Center at the University of South China (Animal Production License No. SYXK 2021-0002). The mice operations conformed to National Laboratory Animal Care and Use Guidelines.

Informed Consent Statement: Not applicable.

Data Availability Statement: The data presented in this study are available from the corresponding author upon reasonable request.

Acknowledgments: We would like to give our sincere appreciation for the help from the Hunan Provincial Key Laboratory for Special Pathogens Prevention and Control Foundation under Grant No. 2014-5, and the Hunan Province Cooperative Innovation Center for Molecular Target New Drug Study (2015-351).

Conflicts of Interest: The authors declare no conflict of interest.

Sample Availability: Samples of TFCO are available from the authors.

References

1. Tong, L.; Huang, S.; Zheng, C.; Zhang, Y.; Chen, Z. Refractory *Mycoplasma pneumoniae* pneumonia in children: Early recognition and management. *J. Clin. Med.* **2022**, *11*, 2824. [[CrossRef](#)] [[PubMed](#)]
2. Lei, W.; Zhou, Z.F.; Jing, C.; Xian, L.S.; Ling, W.X.; Fang, T.L. Pseudomembranous necrotizing laryngotracheobronchitis due to *Mycoplasma pneumoniae*: A case report and literature review. *BMC Infect. Dis.* **2022**, *22*, 183. [[CrossRef](#)] [[PubMed](#)]
3. De Groot, R.C.A.; Meyer Sauter, P.M.; Unger, W.W.J.; van Rossum, A.M.C. Things that could be *Mycoplasma pneumoniae*. *J. Infect.* **2017**, *74*, S95–S100. [[CrossRef](#)]
4. Jiang, Z.; Li, S.; Zhu, C.; Zhou, R.; Leung, P.H.M. *Mycoplasma pneumoniae* infections: Pathogenesis and vaccine development. *Pathogens* **2021**, *10*, 119. [[CrossRef](#)] [[PubMed](#)]
5. Lee, K.L.; Lee, C.M.; Yang, T.L.; Yen, T.Y.; Chang, L.Y.; Chen, J.M.; Lee, P.I.; Huang, L.M.; Lu, C.Y. Severe *Mycoplasma pneumoniae* pneumonia requiring intensive care in children, 2010-2019. *J. Formos. Med. Assoc.* **2021**, *120*, 281–291. [[CrossRef](#)] [[PubMed](#)]
6. Yang, J.; Hooper, W.C.; Phillips, D.J.; Talkington, D.F. Cytokines in *Mycoplasma pneumoniae* infections. *Cytokine Growth Factor Rev.* **2004**, *15*, 157–168. [[CrossRef](#)] [[PubMed](#)]
7. Shimizu, T. Inflammation-inducing factors of *Mycoplasma pneumoniae*. *Front. Microbiol.* **2016**, *7*, 414–421. [[CrossRef](#)]
8. Athamna, A.; Kramer, M.R.; Kahane, I. Adherence of *Mycoplasma pneumoniae* to human alveolar macrophages. *FEMS Immunol. Med. Microbiol.* **1996**, *15*, 135–141. [[CrossRef](#)]
9. Lee, Y.C.; Chang, C.H.; Lee, W.J.; Liu, T.Y.; Tsai, C.M.; Tsai, T.A.; Tsai, C.K.; Kuo, K.C.; Chen, C.C.; Niu, C.K.; et al. Altered chemokine profile in Refractory *Mycoplasma pneumoniae* pneumonia infected children. *J. Microbiol. Immunol. Infect.* **2021**, *54*, 673–679. [[CrossRef](#)]
10. Xue, Y.; Wang, M.; Han, H. Interaction between alveolar macrophages and epithelial cells during *Mycoplasma pneumoniae* infection. *Front. Cell. Infect. Microbiol.* **2023**, *13*, 1052020. [[CrossRef](#)]
11. Tamiya, S.; Yoshikawa, E.; Ogura, M.; Kuroda, E.; Suzuki, K.; Yoshioka, Y. Neutrophil-mediated lung injury both via TLR2-dependent production of IL-1 α and IL-12 p40, and TLR2-independent CARDS toxin after *Mycoplasma pneumoniae* infection in mice. *Microbiol. Spectr.* **2021**, *9*, e0158821. [[CrossRef](#)]

12. Ma, C.; Hao, X.; Gao, L.; Wang, Y.; Shi, J.; Luo, H.; Li, M. Extracellular vesicles released from macrophages infected with *Mycoplasma pneumoniae* stimulate proinflammatory response via the TLR2-NF- κ B/JNK signaling pathway. *Int. J. Mol. Sci.* **2023**, *24*, 8588. [[CrossRef](#)] [[PubMed](#)]
13. Luo, H.; He, J.; Qin, L.; Chen, Y.; Chen, L.; Li, R.; Zeng, Y.; Zhu, C.; You, X.; Wu, Y. *Mycoplasma pneumoniae* lipids license TLR-4 for activation of NLRP3 inflammasome and autophagy to evoke a proinflammatory response. *Clin. Exp. Immunol.* **2021**, *203*, 66–79. [[CrossRef](#)] [[PubMed](#)]
14. Shimizu, T.; Kida, Y.; Kuwano, K. A dipalmitoylated lipoprotein from *Mycoplasma pneumoniae* activates NF-kappa B through TLR1, TLR2, and TLR6. *J. Immunol.* **2005**, *175*, 4641–4646. [[CrossRef](#)] [[PubMed](#)]
15. Quan, W.; Wang, A.; Gao, C.; Li, C. Applications of Chinese *Camellia oleifera* and its by-products: A review. *Front. Chem.* **2022**, *10*, 921246. [[CrossRef](#)]
16. Teixeira, A.M.; Sousa, C. A review on the biological activity of *Camellia* species. *Molecules* **2021**, *26*, 2178. [[CrossRef](#)]
17. Sekine, T.; Arita, J.; Yamaguchi, A.; Saito, K.; Okonogi, S.; Morisaki, N.; Iwasaki, S.; Murakoshi, I. Two flavonol glycosides from seeds of *Camellia sinensis*. *Phytochemistry* **1991**, *30*, 991–995. [[CrossRef](#)]
18. Du, L.C.; Wu, B.L.; Chen, J.M. Flavonoid triglycosides from the seeds of *Camellia oleifera* Abel. *Chin. Chem. Lett.* **2008**, *19*, 1315–1318. [[CrossRef](#)]
19. Gao, D.-F.; Xu, M.; Zhao, P.; Zhang, X.-Y.; Wang, Y.-F.; Yang, C.-R.; Zhang, Y.-J. Kaempferol acetylated glycosides from the seed cake of *Camellia oleifera*. *Food Chem.* **2011**, *124*, 432–436. [[CrossRef](#)]
20. Liu, X.; Jia, L.; Gao, Y.; Li, B.; Tu, Y. Anti-inflammatory activity of total flavonoids from seeds of *Camellia oleifera* Abel. *Acta Biochim. Biophys. Sin.* **2014**, *46*, 920–922. [[CrossRef](#)]
21. Bing, J.; Xu, C.-T.; Li, Q.; Qin, J.-K.; Luo, Y.-W.; Yang, W.G. Chemical constituents of the flavonoids from *Camellia oleifera* and their antiinflammatory activities in vitro. *Chin. Tradit. Pat. Med.* **2019**, *41*, 327–333.
22. Zhang, X.F.; Han, Y.Y.; Di, T.M.; Gao, L.P.; Xia, T. Triterpene saponins from tea seed pomace (*Camellia oleifera* Abel) and their cytotoxic activity on MCF-7 cells in vitro. *Nat. Prod. Res.* **2021**, *35*, 2730–2733. [[CrossRef](#)] [[PubMed](#)]
23. Zhu, L.; Wang, S.; Wan, F.; Zhou, Y.; Wang, Z.; Fan, G.; Wang, P.; Luo, H.; Liao, S.; He, L.; et al. Quantitative analysis of *Camellia oleifera* seed saponins and aqueous two-phase extraction and separation. *Molecules* **2023**, *28*, 2132. [[CrossRef](#)] [[PubMed](#)]
24. Chen, T.; Tang, M.; Zhao, X.R.; Feng, S.L.; Liu, L.; Zhou, L.J.; Cao, X.H.; Huang, Y.; Yang, H.Y.; Ding, C.B. Antioxidant potential evaluation of polysaccharides from *Camellia oleifera* Abel in vitro and in vivo. *Int. J. Biol. Macromol.* **2023**, *248*, 125726. [[CrossRef](#)] [[PubMed](#)]
25. Feng, S.; Tang, M.; Jiang, Z.; Ruan, Y.; Liu, L.; Kong, Q.; Xiang, Z.; Chen, T.; Zhou, L.; Yang, H.; et al. Optimization of extraction process, structure characterization, and antioxidant activity of polysaccharides from different parts of *Camellia oleifera* Abel. *Foods* **2022**, *11*, 3185. [[CrossRef](#)]
26. Xiao, X.; He, L.; Chen, Y.; Wu, L.; Wang, L.; Liu, Z. Anti-inflammatory and antioxidative effects of *Camellia oleifera* Abel components. *Future Med. Chem.* **2017**, *9*, 2069–2079. [[CrossRef](#)] [[PubMed](#)]
27. Zhu, W.F.; Wang, C.L.; Ye, F.; Sun, H.P.; Ma, C.Y.; Liu, W.Y.; Feng, F.; Abe, M.; Akihisa, T.; Zhang, J. Chemical constituents of the seed cake of *Camellia oleifera* and their antioxidant and antimelanogenic activities. *Chem. Biodivers.* **2018**, *15*, e1800137. [[CrossRef](#)]
28. Qiu, Y.; He, D.; Yang, J.; Ma, L.; Zhu, K.; Cao, Y. Kaempferol separated from *Camellia oleifera* meal by high-speed countercurrent chromatography for antibacterial application. *Eur. Food Res. Technol.* **2020**, *246*, 2383–2397. [[CrossRef](#)]
29. Ko, J.; Yeh, W.J.; Huang, W.C.; Yang, H.Y. *Camellia oleifera* seed extract mildly ameliorates carbon tetrachloride-induced hepatotoxicity in rats by suppressing inflammation. *J. Food Sci.* **2019**, *84*, 1586–1591. [[CrossRef](#)]
30. Yeh, W.J.; Ko, J.; Huang, W.C.; Cheng, W.Y.; Yang, H.Y. Crude extract of *Camellia oleifera* pomace ameliorates the progression of non-alcoholic fatty liver disease via decreasing fat accumulation, insulin resistance and inflammation. *Br. J. Nutr.* **2020**, *123*, 508–515. [[CrossRef](#)]
31. Chen, L. Extraction and Separation, Chemical Structure Characterization and Biological Activity of Flavonoid Glycosides in *Camellia oleifera* Seed Cake. *Masters' Thesis*, Nanchang University, Nanchang, China, 2011.
32. Waites, K.B.; Xiao, L.; Liu, Y.; Balish, M.F.; Atkinson, T.P. *Mycoplasma pneumoniae* from the respiratory tract and beyond. *Clin. Microbiol. Rev.* **2017**, *30*, 747–809. [[CrossRef](#)]
33. Chung, M.J.; Pandey, R.P.; Choi, J.W.; Sohng, J.K.; Choi, D.J.; Park, Y.I. Inhibitory effects of kaempferol-3-O-rhamnoside on ovalbumin-induced lung inflammation in a mouse model of allergic asthma. *Int. Immunopharmacol.* **2015**, *25*, 302–310. [[CrossRef](#)] [[PubMed](#)]
34. Medeiros, K.C.; Faustino, L.; Borduchi, E.; Nascimento, R.J.; Silva, T.M.; Gomes, E.; Piuvezam, M.R.; Russo, M. Preventive and curative glycoside kaempferol treatments attenuate the TH2-driven allergic airway disease. *Int. Immunopharmacol.* **2009**, *9*, 1540–1548. [[CrossRef](#)] [[PubMed](#)]
35. Yu, L.; Chen, C.; Wang, L.F.; Kuang, X.; Liu, K.; Zhang, H.; Du, J.R. Neuroprotective effect of kaempferol glycosides against brain injury and neuroinflammation by inhibiting the activation of NF-kappaB and STAT3 in transient focal stroke. *PLoS ONE* **2013**, *8*, e55839. [[CrossRef](#)]
36. Lin, Y.; Tan, D.; Kan, Q.; Xiao, Z.; Jiang, Z. The protective effect of naringenin on airway remodeling after *Mycoplasma pneumoniae* infection by inhibiting autophagy-mediated lung inflammation and fibrosis. *Mediat. Inflamm.* **2018**, *2018*, 1–10. [[CrossRef](#)]

37. Tang, J.; Li, Y.; Wang, J.; Wu, Q.; Yan, H. Polydatin suppresses the development of lung inflammation and fibrosis by inhibiting activation of the NACHT domain-, leucine-rich repeat-, and pyd-containing protein 3 inflammasome and the nuclear factor- κ B pathway after *Mycoplasma pneumoniae* infection. *J. Cell. Biochem.* **2018**, *120*, 10137–10144. [[CrossRef](#)]
38. Li, G.; Fan, L.; Wang, Y.; Huang, L.; Wang, M.; Zhu, C.; Hao, C.; Ji, W.; Liang, H.; Yan, Y.; et al. High co-expression of TNF- α and CARDS toxin is a good predictor for refractory *Mycoplasma pneumoniae* pneumonia. *Mol. Med.* **2019**, *25*, 38–47. [[CrossRef](#)] [[PubMed](#)]
39. Ding, Y.; Chu, C.; Li, Y.; Li, G.; Lei, X.; Zhou, W.; Chen, Z. High expression of HMGB1 in children with refractory *Mycoplasma pneumoniae* pneumonia. *BMC Infect. Dis.* **2018**, *18*, 439. [[CrossRef](#)] [[PubMed](#)]
40. Wu, P.; Wang, J. Changes and significance of serum sB7-H3 and cytokines in children with *Mycoplasma pneumoniae* pneumonia. *J. Coll. Physicians Surg. Pak.* **2020**, *30*, 268–271. [[CrossRef](#)] [[PubMed](#)]
41. Fang, Y.; Wang, H.; Xia, X.; Yang, L.; He, J. Kaempferol 3-O-(2G-glucosylrutinoside)-7-O-glucoside isolated from the flowers of *Hosta plantaginea* exerts anti-inflammatory activity via suppression of NF- κ B, MAPKs and Akt pathways in RAW 264.7 cells. *Biomed. Pharmacother.* **2022**, *153*, 113295–113301. [[CrossRef](#)] [[PubMed](#)]
42. Fang, S.H.; Rao, Y.K.; Tzeng, Y.M. Inhibitory effects of flavonol glycosides from *Cinnamomum osmophloeum* on inflammatory mediators in LPS/IFN- γ -activated murine macrophages. *Bioorg. Med. Chem.* **2005**, *13*, 2381–2388. [[CrossRef](#)] [[PubMed](#)]
43. Shimizu, T.; Kida, Y.; Kuwano, K. Triacylated lipoproteins derived from *Mycoplasma pneumoniae* activate nuclear factor- β through toll-like receptors 1 and 2. *Immunology* **2007**, *121*, 473–483. [[CrossRef](#)]
44. Chu, H.W.; Jeyaseelan, S.; Rino, J.G.; Voelker, D.R.; Wexler, R.B.; Campbell, K.; Harbeck, R.J.; Martin, R.J. TLR2 signaling is critical for *Mycoplasma pneumoniae*-induced airway mucin expression. *J. Immunol.* **2005**, *174*, 5713–5719. [[CrossRef](#)] [[PubMed](#)]
45. Takeuchi, O.; Kaufmann, A.; Grote, K.; Kawai, T.; Hoshino, K.; Morr, M.; Mühlradt, P.F.; Akira, S. Cutting edge: Preferentially the R-stereoisomer of the mycoplasmal lipopeptide macrophage-activating lipopeptide-2 activates immune cells through a toll-like receptor 2- and MyD88-dependent signaling pathway. *J. Immunol.* **2000**, *164*, 554–557. [[CrossRef](#)] [[PubMed](#)]
46. Hirao, S.; Wada, H.; Nakagaki, K.; Saraya, T.; Kurai, D.; Mikura, S.; Yasutake, T.; Higaki, M.; Yokoyama, T.; Ishii, H.; et al. Inflammation provoked by *Mycoplasma pneumoniae* extract: Implications for combination treatment with clarithromycin and dexamethasone. *FEMS Immunol. Med. Microbiol.* **2011**, *62*, 182–189. [[CrossRef](#)]
47. Ye, Y.; Fang, F.; Li, Y. Isolation of the sapogenin from defatted seeds of *Camellia oleifera* and its neuroprotective effects on dopaminergic neurons. *J. Agric. Food Chem.* **2014**, *62*, 6175–6182. [[CrossRef](#)]
48. Ye, Y.; Xing, H.; Chen, X. Anti-inflammatory and analgesic activities of the hydrolyzed sasanquasaponins from the defatted seeds of *Camellia oleifera*. *Arch. Pharm. Res.* **2013**, *36*, 941–951. [[CrossRef](#)]
49. Hou, C.; Chen, L.; Yang, L.; Ji, X. An insight into anti-inflammatory effects of natural polysaccharides. *Int. J. Biol. Macromol.* **2020**, *153*, 248–255. [[CrossRef](#)] [[PubMed](#)]
50. Simpson, M.E.; Petri, W.A. TLR2 as a therapeutic target in bacterial infection. *Trends Mol. Med.* **2020**, *26*, 715–717. [[CrossRef](#)] [[PubMed](#)]

Disclaimer/Publisher's Note: The statements, opinions and data contained in all publications are solely those of the individual author(s) and contributor(s) and not of MDPI and/or the editor(s). MDPI and/or the editor(s) disclaim responsibility for any injury to people or property resulting from any ideas, methods, instructions or products referred to in the content.